Constraints on 5*f*-electron magnetism in Ga-stabilized δ-Pu from x-ray magnetic circular dichroism

Alexander A. Baker [1], Gilberto Fabbris [2], Daniel Haskel [2], and Jason R. Jeffries [1]
[1] *Lawrence Livermore National Laboratory, Livermore, California 94550, USA*
[2] *Lemont Advanced Photon Source, Argonne National Laboratory, Lemont, Illinois 60439, USA*

(Received 29 April 2024; revised 22 July 2024; accepted 16 August 2024; published 10 September 2024)

Density-functional theory models of δ-Pu accurately predict crystal structure, phonon density of states, and unit cell volumes but require magnetic degrees of freedom which have never been experimentally verified. Some models invoke an on-site cancellation of spin and orbital moments, engendering a near-zero bulk magnetization, undetectable by most probes. Here, we employ x-ray magnetic circular dichroism at the Pu $M_{4,5}$ edges to directly probe spin and orbital moments using the magneto-optical sum rules. The data show no dichroism within experimental error, constraining polarized moments at 6 T and 3 K to $\mu_{L,S} < 0.1\mu_B$. These experiments point to the absence of even unconventional spin-orbit compensated order in δ-Pu.

DOI: 10.1103/PhysRevB.110.104417

I. INTRODUCTION

Since its discovery in 1940, plutonium has had an outsized influence on global events as a weapon of war and deterrent, as a national security fulcrum, as a source of carbon-free power, and as a vehicle to power exploration beyond the solar system. Despite the importance of these applications, our fundamental understanding of Pu lags far behind all other macroscopically available elements, due to the logistical difficulty of performing experiments, and the rich complexity of its electronic structure. Modern theories of Pu face challenges in reproducing the narrow free-energy landscape and structural properties of the unprecedented six ambient-pressure phases of this element. Major progress was made in the early 2000s when valence and magnetic degrees of freedom were considered within dynamical mean-field theory (DMFT) [1,2] and density-functional theory (DFT) [3–5]. Both frameworks had significant success in predicting observed phenomena including structural phase transformations or photoemission spectra; however, the theories were distinguished by disparate magnetic behavior. Early DFT models invoked magnetic ordering to better predict observed properties, and while this was a victory for predictive theory for Pu, this proposition also ignited a major controversy: Pu was known to be experimentally nonmagnetic; it had been shown to preclude magnetic order and classical local moment behavior in the bulk, instead showing only an enhanced Pauli paramagnetic response [6].

In recent years, refinements of the DFT model have settled on a description of Pu lacking a bulk magnetization, but still requiring magnetic degrees of freedom. The lack of magnetic ordering is proposed to be driven by a nearly complete on-site cancellation of the spin and orbital moments, both of order $3\mu_B$, of the *5f* electronic states in Pu [3]. This near-net-zero moment cancellation theory still predicts the temperature-dependent structures of Pu, reproduces the phonon spectra [7–9], and remains consistent with existing bulk magnetic measurements due to the small on-atom net moment. DMFT approaches, conversely, do not require canceling orbital and spin moments and instead involve mixed or fluctuating valence states [10,11], where the magnetic moment is not missing but rather undetected by laboratory techniques, and can be revealed through neutron spectroscopy [12]. In light of these competing models it is important to provide a direct test of the DFT's prediction of on-site cancellation, which cannot be refuted or confirmed with conventional bulk probes of magnetization, leaving a key conjecture of the model without validation.

X-ray magnetic circular dichroism (XMCD), as a tool to measure spin and orbital moments *separately* through the magneto-optical sum rules, is uniquely suited to resolve this question of near-net-zero moment cancellation in Pu [13–16]. A corollary near-net-zero moment system is ferromagnetic Gd-doped $SmAl_2$, for which the Sm^{3+} ion exists with equal and opposite spin and orbital $4f$ moments of order $1\mu_B$/Sm. $Sm_{0.974}Gd_{0.026}Al_2$ has been experimentally verified to have a vanishing bulk moment while also evincing substantial XMCD at the Sm $M_{4,5}$ edges [17]. Similarly, UFe_2 has been shown to host on-site cancellation of $5f$ moments through XMCD measurements at the $M_{4,5}$ and $N_{4,5}$ edges [18,19] corroborating earlier neutron scattering experiments [20]. Near-cancellation of spin and orbital moments has also been shown in $[UF_6]^{2-}$, where a small net moment belies relatively large individual contributions [21].

The ferromagnetic compound PuSb has, well below its Curie temperature, a net saturation moment of $0.68\mu_B$/Pu at 5 K [22]. Low-temperature x-ray spectroscopy measurements on PuSb in a magnetic field $H = 50$ mT at the Pu $M_{4,5}$ edges reveal very large XMCD signals corresponding to spin and orbital *5f* moments of -2.0 and $2.8\mu_B$/Pu, respectively, despite the modest saturation moment. Similarly, XMCD measurements on the unconventional superconductor $PuCoGa_5$ [23] yielded XMCD on the order of ∼3% against spin and orbital *5f* moments of -0.04 and $0.068\mu_B$/Pu, albeit in a 17 T field. The field-polarized moment of δ-Pu is constrained by muon spin relaxation and superconducting quantum interference device (SQUID) magnetometry to be $\sim 0.005\mu_B$/Pu at $H = 6$ T [24–26], a factor of at least 100 smaller than the saturation magnetization of PuSb. However, even with such a small,

polarized moment in Pu, the predicted large, antialigned, on-site spin and orbital moments from the DFT model would still be expected to manifest measurable Pu M_4-edge XMCD signals, which are large when the (effective, which includes magnetic dipole contribution [22,27]) spin and orbital moments have large values with opposite sign, as predicted by Ref. [3]. If such moments are not present, then SQUID measurements of susceptibility would suggest that the XMCD signal would be very small, below the detection limits achievable with the current experimental configuration. In this study, Pu $M_{4,5}$-edge XMCD measurements of Ga-stabilized δ-Pu allowed constraining the orbital and spin moments by comparison with the experimental noise level, leading to values below $0.1\mu_B$/Pu at 6 T and 3 K.

II. EXPERIMENTAL

A homogenized, face-centered cubic δ-phase Pu-0.6 wt. % Ga alloy (phase confirmed by density measurements) was polished to a right cylinder of 3-mm diameter and 100-μm thickness according to established metallographic procedures for δ-phase Pu. An approximately 200-μm-diameter hole was laser drilled in the center of the polished specimen to serve as an alignment fiducial. The sample was then contained in a hermetically sealed sample holder comprising two layers of Be windows (25 and 50 μm thick) and one layer of Kapton window (50 μm thick) to minimize x-ray attenuation from the specimen holder at the $M_{4,5}$ edges (3.7–4 keV). The sample showed no evidence of oxidation or surface degradation, confirming the quality of the seals. Measurements were conducted at beamline 4-ID-D of the Advanced Photon Source, Argonne National Laboratory. The sample holder was mounted in a Cu clamp inside the variable temperature insert of a superconducting magnet and cooled by ^{4}He vapor. The sample was cooled to base temperature (∼3 K), then a magnetic field of 6 T was applied parallel to the incident x-ray beam direction. Fluorescence yield spectra were acquired using a four-element silicon drift diode detector placed at 90 ° to the incoming beam—the sample was oriented at 45 ° to the incident beam. The incident x rays were circularly polarized using a diamond phase plate, and incident intensity (I_0) was measured immediately upstream of the magnet. X-ray absorption spectra (XAS) data were collected by switching x-ray helicity at every energy step to minimize drift and enable point-by-point XMCD. The applied field was flipped approximately every 12 h to collect data with field along and opposite to the x-ray helicity vector. The lower-energy M_5 edge exhibited a higher noise level due to increased self-attenuation of fluorescent photons, as well as a lower expected XMCD signal, which is proportional to the sum of the effective spin and orbital moments (which is near zero in the cancellation scheme, if the magnetic dipole contribution is neglected). For this reason, more time was spent acquiring data at M_5; ultimately, data at M_5 were accumulated for approximately 80 h, while data at M_4 were accumulated for 20 h, yielding a total of 100 h of beam-on-sample. Ultimately, this scheme resulted in approximately 20 000 integrated counts at the white line of the M_5 edge, and 80 000 at M_4. The averaged spectra for each helicity were normalized to I_0, then a linear preedge background was subtracted. The edge steps across the $M_{4,5}$ edges were scaled to unity prior to the self-absorption corrections.

III. RESULTS AND DISCUSSION

Figure 1 shows the uncorrected XAS, derived from the fluorescence signal of the sample by normalizing the fluorescence to the incident beam intensity and subtracting a linear background. In addition, Fig. 1 displays the XMCD signals computed from the difference of the positive- and negative-helicity XAS at the M_4 and M_5 edges. Despite this strong, clean signal, the XMCD spectra show no overt evidence of magnetic dichroism outside of the noise. The jump seen in Fig. 1(b) around 3.987 keV is due to a glitch in the monochromator, rather than originating in the sample. The lack of a detectable XMCD signal is somewhat unexpected based on an on-site cancellation model, wherein large moments would lead to large XMCD, even if the net moment is zero. While it is possible that a small XMCD signal is contained within the noise, such a signal would be driven by small spin and orbital moments, and thus inconsistent with the magnitude of magnetic moments required by theory to produce the energy level splitting that matches the observed crystalline densities. However, corrections for self-absorption of fluorescence photons must be conducted before this can be conclusively stated.

Analysis of fluorescence data for bulk samples of high-Z materials must take into account self-absorption effects, as fluorescence x rays emitted can be reabsorbed within the sample before reaching the detector. This effect is most pronounced around the absorption edge, which can lead to significant modification of the XAS signal. The self-absorption correction is performed using the equation [28]

$$I_{\text{cor}} = \frac{N\left[\frac{\mu_{tf}}{\mu_e}\frac{\sin\theta_i}{\sin\theta_f} + \frac{\mu_b}{\Delta\mu_e}\right]}{\left[\frac{\mu_{tf}}{\Delta\mu_e}\frac{\sin\theta_i}{\sin\theta_f} + \frac{\mu_b}{\Delta\mu_e} + 1\right] - N}, \tag{1}$$

where I_{cor} is the absorption-corrected XAS intensity, N the background subtracted edge-step normalized fluorescence data (e.g., that of Fig. 1), μ_{tf} is the weighted total absorption cross section of all atoms in the sample at the specific fluorescence energy (M_α or M_β of Pu in this case), $\Delta\mu_e$ is the absorption cross section of the central atom (Pu) across the absorption edge, μ_B is the absorption cross section of all atoms (Pu and Ga) below the absorption edge, θ_i is the angle of x-ray incidence relative to the sample surface, and θ_f is the angle between the sample surface and the detected emitted photon wave vector. In our experimental geometry, $\theta_i = \theta_f = 45^\circ$, so the geometric terms containing these parameters cancel to unity. The edge-step ratio of the absorption-corrected data for spin-orbit split $M_{5,4}$ edges was scaled according to the tabulated absorption cross sections, i.e., $\Delta\mu_e(M_4)/\Delta\mu_e(M_5) = 0.61$, with M_4 scaled immediately before the glitch around 3985 eV. All cross sections are taken from the XCOM photon cross-section database [29].

The absorption-corrected XAS and XMCD data are plotted in Figs. 1(c) and 1(d), displaying significant enhancement of the peak strength around the white line compared to the uncorrected data of Figs. 1(a) and 1(b). A complication of such corrections is that they can also lead to magnification of

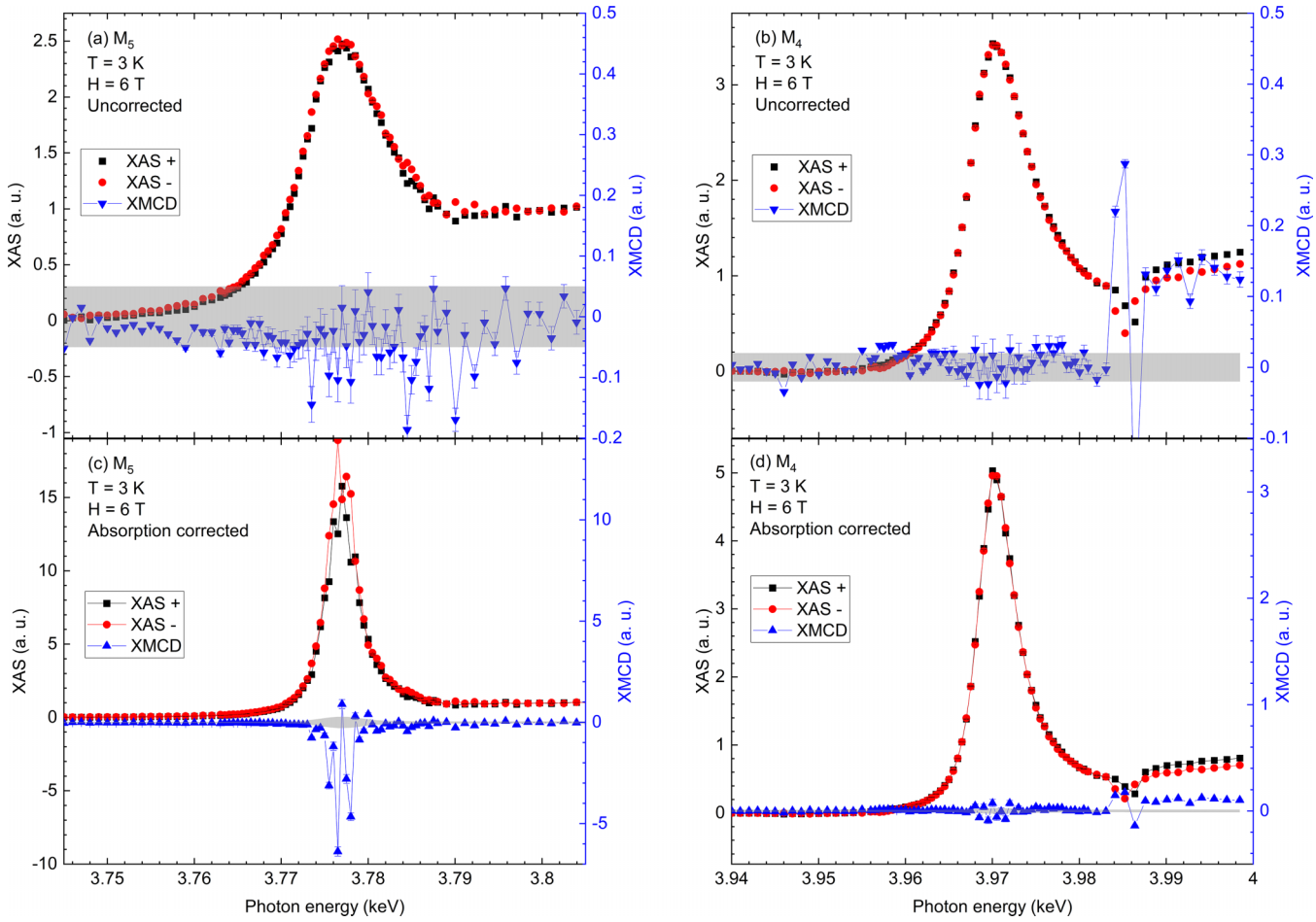

FIG. 1. Uncorrected XAS and XMCD data collected in fluorescence yield mode at the M_5 (a) and M_4 (b) absorption edges of Pu. Note that XMCD is plotted on an expanded scale on the right axis. No dichroism is observed above the noise floor; error bars (comparable to point size in most cases) arise from counting statistics propagated through data analysis. Applying the self-absorption correction yields the modified spectra presented in (c) and (d). The nonlinear nature of the correction greatly enhances small differences around the peak of the absorption edge. The scattered points around the M_5 edge could indicate the development of XMCD (albeit with an unusual local structure), but any dichroism at the M_4 edge remains small, and would be expected to be of comparable size to the XMCD for PuSb. Solid gray regions indicate an approximate noise band based on scatter of data, which is then scaled according to the self-absorption correction scaling factors of the XAS, causing an energy-dependent expansion of noise.

noise in the data [presented as the gray band from Figs. 1(a) and 1(b) projected via the energy-dependent scaling of Eq. (1) into Figs. 1(c) and 1(d)] as well as experiencing extreme divergence when the raw fluorescence approaches specific values, because of the presence of N in the denominator of Eq. (1). This magnification of noise is particularly prominent in Fig. 1(c) around the M_5 absorption edge, which displays exaggerated point-to-point variance between adjacent energy points in the XMCD data. The validity of these corrections can be confirmed by calculating the branching ratio (B), defined as the integrated area of the M_5 XAS peak divided by the integrated area of the M_4 and M_5 peaks. The data here yields $B = 0.84$, which is in close agreement with values determined at the $N_{4,5}$ edges using electron-energy-loss spectroscopy [30], as well as XAS measurements on PuSb [22]. This value matches that produced by an intermediate coupling scheme [31] and is much closer to that expected from a jj coupling scheme, rather than a Hund's rule ground state, consistent with strong spin-orbit coupling that splits the $5f$ band. Inferred dichroism spectra from the amplified noise in Fig. 1(c) or 1(d), however, do not resemble data gathered on other Pu compounds and would likely require an exotic multiplet configuration to reproduce any inferred energy dependence; this is especially unlikely for an fcc lattice that has only one crystallographic site [22]. The M_4 edge has a similar amplified noise, though with smaller magnitude than that at M_5. This is due to the higher data quality at M_4 and the self-absorption correction being less sensitive in that energy region. Even with the self-absorption correction, the experimental XMCD spectra at M_4 or M_5 do not exhibit unambiguous dichroism above the noise level, though presumably some small signal due to paramagnetic susceptibility should be present below experimental detection thresholds. With the present noise level, it is not possible to assess the contributions of spin and orbital moments to the paramagnetic susceptibility.

Given the lack of clear magnetic dichroism in Fig. 1, it is instructive to use the available information to perform a simple bounding exercise to constrain the magnitude of any

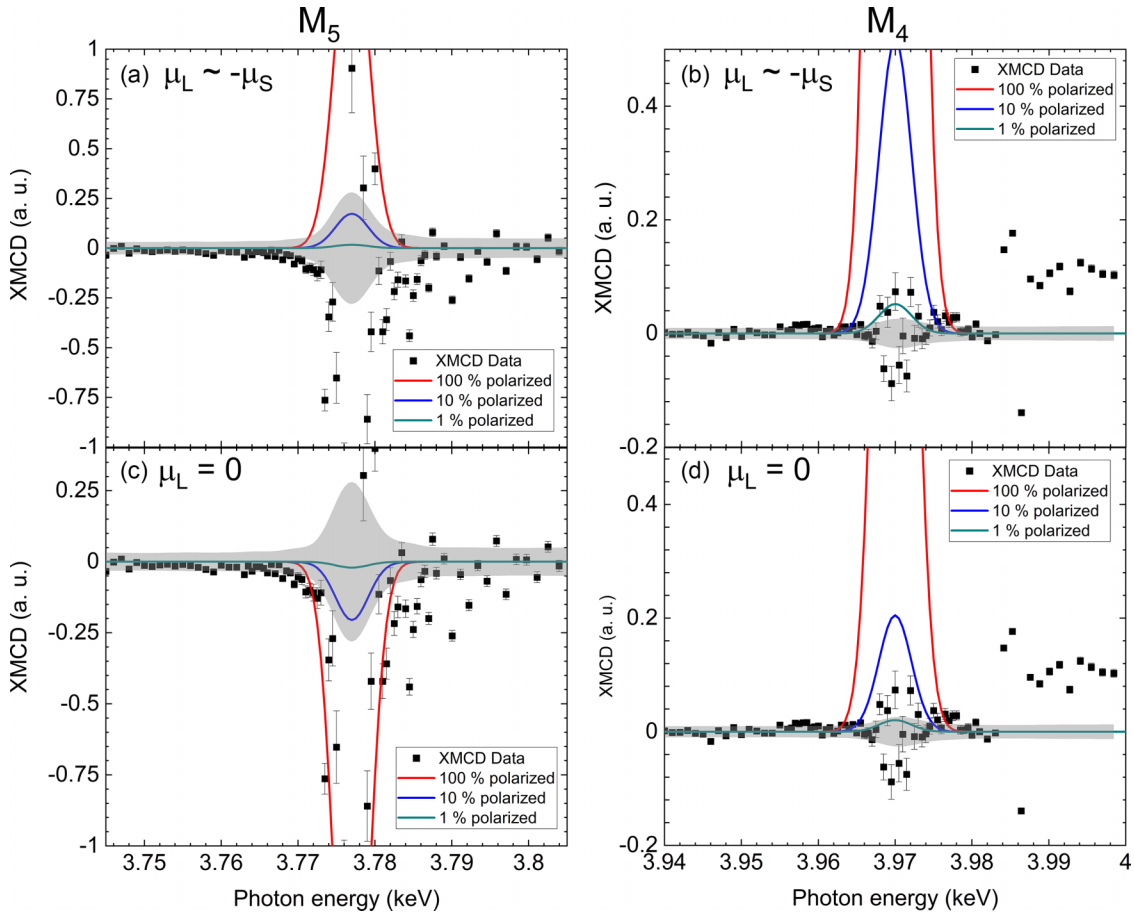

FIG. 2. XMCD spectra collected at the M_5 (a),(c) and M_4 (b),(d) edges (black points, taken from Fig. 1 and expanded for M_5), plotted with solid lines indicating the approximate expected spectra (Gaussians of areas dictated by the magneto-optical spin-orbit sum rules) that would result from values $\mu_S = 3.4\mu_B$, $\mu_L = -3.0\mu_B$ with moments fully polarized, 10% polarized (saturation field = 600 T), and 1% polarized (saturation field = 600 T). These correspond to the near equal and opposite values of spin and orbital moments that arise from the on-site cancellation model (a),(b), as well as the purely spin moment that arises from the case of quenched orbital moments and fully delocalized electrons (c),(d). In all cases it is clear that the moments are not fully polarized, with the sensitive M_4 edge enforcing at most 1% polarization ($\mu_S = 0.034\mu_B$). This places heavy constraints on the possible configurations of magnetic moments in δ-Pu, in contrast to many theoretical works, but matching well with other direct and indirect experimental probes of magnetism in Pu. Shaded areas indicate an estimate of the scatter in the uncorrected XAS data, projected through the self-absorption correction. Error bars arise from counting statistics.

$5f$ magnetic moment in δ-Pu that can be hidden within the noise floor of the experiment. The magneto-optical sum rules, which enable extraction of the orbital moment, $\langle L_z \rangle$, and effective spin polarization, $\langle S_{\text{eff}} \rangle$, are given as [13,14,32]

$$-\mu_L = \langle L_z \rangle = n_h \frac{\Delta I_{M_5} + \Delta I_{M_4}}{I_{M_5} + I_{M_4}} \tag{2}$$

and

$$-\frac{\mu_{S,\text{eff}}}{2} = \langle S_{\text{eff}} \rangle = \langle S_Z \rangle + 3\langle T_Z \rangle = \left(\frac{n_h}{2}\right) \frac{\Delta I_{M_5} - \frac{3}{2}\Delta I_{M_4}}{I_{M_5} + I_{M_4}}, \tag{3}$$

where n_h is the number of holes in the $5f$ shell (8.6/Pu) [30,33], $\Delta I_{M_{5,4}}$ the integrated area of the XMCD at the $M_{5,4}$ edges, $I_{M_{5,4}}$ the integrated area of the XAS at the $M_{5,4}$ edges, $\langle L_z \rangle$ the orbital angular momentum, $\langle S_z \rangle$ the spin angular momentum, and $\langle T_z \rangle$ the magnetic dipole contribution. The magneto-optical sum rules can be rearranged to provide estimates of the expected area of the XMCD at the $M_{4,5}$ absorption edges based on the measured integrated area of the XAS, known values of n_h, and predictions for $\mu_{L,S}$ from the near-net-zero, on-site cancellation DFT model [3]. A value of $-0.13\mu_B$/Pu was chosen for $\langle T_z \rangle$, based on previous XMCD studies of PuSb [22]. The degree of polarization and balance of spin and orbital terms determines signal size, $\langle T_z \rangle$ provides a correction on the order of 10% when changed from 0 to $-0.13\mu_B$/Pu, and less than 5% when increased to the value of 0.06 determined for $PuFe_2$ [27]. A negative $\langle T_z \rangle$ implies more localized electrons, which aligns with the proposed magnetic configuration. For this exercise we approximate the peaks in the dichroism spectra as Gaussians with areas dictated by the values of $\Delta I_{M_{5,4}}$ determined by rearranging Eqs. (2) and (3). While this approximation is not strictly accurate and ignores details of atomic multiplet configurations, it is likely constraining to the order of magnitude.

The results of this approximation are plotted in Fig. 2 for two cases: on-site self-cancellation (a),(b) and fully quenched orbital moments (c),(d) (note that the M_5 data is zoomed in to

show the small predicted signals). Here we take $\mu_S = 3.4\mu_B$ and $\mu_L = -3.0\mu_B$ from [3] (yielding a saturation magnetization of $0.4\mu_B$) and estimate the signal that would arise if the sample were fully polarized (note that Pu is known to not be fully polarized at 6 T [24]), 10% polarized (saturation field = 60 T), and 1% polarized (saturation field = 600 T). The large noise envelope at the M_5 edge challenges strong constraints on the $5f$ magnetic moments, although full polarization of the Pu moments is highly implausible. Significantly stronger constraints are imposed when considering both edges, which is required for the sum rules. At the M_4 edge, the higher data quality clearly indicates that the cases of 100% and 10% polarization are incompatible with the measured results for both on-site cancellation and fully quenched orbital moments. The small signal arising from 1% polarization ($\mu_S = 0.004\mu_B$) cannot be excluded with the acquired data, with the noise envelope suggesting that less than 2% of the predicted total moment is accessible at these fields, implying a saturation field in excess of 300 T. These limits on magnetization in a 6 T field yield less than 5 μeV of Zeeman energy, well less than the 20 meV that separates α- and δ-Pu [5]. Magnetometry of δ-Pu confirms that the saturation field is greater than 6 T [24], but data at significantly higher fields are not available. Rare earth–doped Pd samples have been reported to have saturation fields in excess of 20 T [34], but no reports exist of saturation above 100 T. A high saturation field fits with an enhanced Pauli paramagnetic response [6], where fields in the kilotesla range are required to reach such magnetizations. These results therefore place strict limits on the near-net-zero magnetic cancellation DFT model for the electronic structure of δ-Pu, demonstrating a need for predictions of field-dependent magnetism, and experiments to test them. While these measurements cannot rule out on-site cancellation of moments with a very high saturation field, they do suggest that the energy associated with magnetic order at low fields does not compare with phase transformations above room temperature that Pu demonstrates. Even if ordered magnetism is found at high fields, it appears to not provide the degrees of freedom required for DFT to make accurate predictions of plutonium's physical properties.

The simple model of fully quenched orbital moments with large spin moments is similarly challenged by these data, again requiring saturation fields in the range of hundreds of tesla. The possibility of fully quenched orbital moments, $\mu_L = 0\mu_B$, is therefore precluded for $\mu_S > 0.1\mu_B$, which would be the case if δ-Pu were a purely spin-only magnetic system (and would also be incompatible with the measured branching ratio of 0.84).

IV. CONCLUSION

These results thus place significant new constraints on the presence of polarized moments in δ-Pu yet are consistent with several decades of experimental work that has failed to find any evidence of conventional, ordered magnetism. XMCD allows the resolution of spin and orbital contributions to magnetic moments and based upon the absence of dichroism in these experiments and the measured noise level, we are able to place strict limits on the individual contributions to the magnetic moments. The spin and orbital moments must be less than $0.1\mu_B$ at 6 T, and likely much less, meaning that the moments are not more than 2% polarized. This implies a saturation field in excess of 300 T at 3 K, significantly larger than anything observed in comparable systems. This finding suggests a clear need for improved DFT frameworks to treat magnetic degrees of freedom in δ-Pu, and high-field measurements to test them, as well as providing indirect support for DMFT models. We note that magnetism included in electronic structure theories provides degrees of freedom that are required to accurately reproduce physical quantities such as Young's modulus, crystalline structures, and lattice parameters. The fact that these predictions yield descriptions of Pu that are compatible with observable data suggests that some energy splitting exists within the electronic structure of δ-Pu, but the preponderance of experimental data, now including individual limits on orbital and spin magnetic moments, strongly suggests that magnetism may not be the sole progenitor of this energy splitting.

ACKNOWLEDGMENTS

This work was performed under the auspices of the U.S. Department of Energy by Lawrence Livermore National Laboratory under Contract No. DE-AC52-07NA27344. This research used the Advanced Photon Source, a U.S. Department of Energy (DOE) Office of Science user facility operated for the DOE Office of Science by Argonne National Laboratory under Contract No. DE-AC02-06CH11357.

[1] G. Kotliar, S. Y. Savrasov, K. Haule, V. S. Oudovenko, O. Parcollet, and C. A. Marianetti, Electronic structure calculations with dynamical mean-field theory, Rev. Mod. Phys. **78**, 865 (2006).

[2] S. Y. Savrasov, G. Kotliar, and E. Abrahams, Correlated electrons in δ-plutonium within a dynamical mean-field picture, Nature (London) **410**, 793 (2001).

[3] P. Söderlind, Cancellation of spin and orbital magnetic moments in δ-Pu: Theory, J. Alloys Compd. **444**, 93 (2007).

[4] P. Söderlind, F. Zhou, A. Landa, and J. E. Klepeis, Phonon and magnetic structure in δ-plutonium from density-functional theory, Sci. Rep. **5**, 15958 (2015).

[5] P. Söderlind and B. Sadigh, Density-functional calculations of α, β, γ, δ, δ', and ϵ plutonium, Phys. Rev. Lett. **92**, 185702 (2004).

[6] J. C. Lashley, A. Lawson, R. J. McQueeney, and G. H. Lander, Absence of magnetic moments in plutonium, Phys. Rev. B **72**, 054416 (2005).

[7] P. Söderlind, Lattice dynamics and elasticity for ε-plutonium, Sci. Rep. **7**, 1116 (2017).

[8] P. Söderlind, A. Landa, J. E. Klepeis, Y. Suzuki, and A. Migliori, Elastic properties of Pu metal and Pu-Ga alloys, Phys. Rev. B **81**, 224110 (2010).

[9] J. Wong, M. Krisch, D. L. Farber, F. Occelli, A. J. Schwartz, T.-C. Chiang, M. Wall, C. Boro, and R. Xu, Phonon dispersions of fcc δ-plutonium-gallium by inelastic x-ray scattering, Science **301**, 1078 (2003).

[10] A. B. Shick, J. Kolorenc, J. Rusz, P. M. Oppeneer, A. I. Lichtenstein, M. I. Katsnelson, and R. Caciuffo, Unified character of correlation effects in unconventional Pu-based superconductors and δ-Pu, Phys. Rev. B **87**, 020505(R) (2013).

[11] J. H. Shim, K. Haule, and G. Kotliar, Fluctuating valence in a correlated solid and the anomalous properties of δ-plutonium, Nature (London) **446**, 513 (2007).

[12] M. Janoschek, P. Das, B. Chakrabarti, D. L. Abernathy, M. D. Lumsden, J. M. Lawrence, J. D. Thompson, G. H. Lander, J. N. Mitchell, S. Richmond *et al.*, The valence-fluctuating ground state of plutonium, Sci. Adv. **1**, e1500188 (2015).

[13] P. Carra, B. T. Thole, M. Altarelli, and X. Wang, X-ray circular dichroism and local magnetic fields, Phys. Rev. Lett. **70**, 694 (1993).

[14] B. T. Thole, P. Carra, F. Sette, and G. van der Laan, X-ray circular dichroism as a probe of orbital magnetization, Phys. Rev. Lett. **68**, 1943 (1992).

[15] G. van der Laan, Applications of soft x-ray magnetic dichroism, J. Phys.: Conf. Ser. **430**, 012127 (2013).

[16] G. van der Laan and K. T. Moore, *Magnetism and Synchrotron Radiation*, Springer Proceedings in Physics, edited by E. Beaurepaire, H. Bulou, F. Scheurer, and J.-P. Kappler (Springer, Berlin, Heidelberg 2010), Vol. 133, Chap. 11, pp. 313–344.

[17] S. S. Dhesi, G. van der Laan, P. Bencok, N. B. Brookes, R. M. Galéra, and P. Ohresser, Spin- and orbital-moment compensation in the zero-moment ferromagnet $Sm_{0.974}Gd_{0.026}Al_2$, Phys. Rev. B **82**, 180402(R) (2010).

[18] M. Finazzi, P. Sainctavit, A. M. Dias, J. P. Kappler, G. Krill, J. P. Sanchez, P. Dalmas de Réotier, A. Yaouanc, A. Rogalev, and J. Goulon, X-ray magnetic circular dichroism at the U $M_{4,5}$ absorption edges of UFe_2, Phys. Rev. B **55**, 3010 (1997).

[19] T. Okane, Y. Takeda, S.-I. Fujimori, K. Terai, Y. Saitoh, Y. Muramatsu, A. Fujimori, Y. Haga, E. Yamamoto, and Y. Ōnuki, Soft x-ray magnetic circular dichroism study of UFe_2, Phys. B (Amsterdam, Neth.) **378–380**, 959 (2006).

[20] G. H. Lander, M. S. S. Brooks, and B. Johansson, Orbital band magnetism in actinide intermetallics, Phys. Rev. B **43**, 13672 (1991).

[21] K. S. Pedersen, K. R. Meihaus, A. Rogalev, F. Wilhelm, D. Aravena, M. Amoza, E. Ruiz, J. R. Long, J. Bendix, and R. Clérac, $[UF_6]^{2-}$: A molecular hexafluorido actinide(IV) complex with compensating spin and orbital magnetic moments, Angew. Chem., Int. Ed. **58**, 15650 (2019).

[22] M. Janoschek, D. Haskel, J. Fernandez-Rodriguez, M. van Veenendaal, J. Rebizant, G. H. Lander, J. X. Zhu, J. D. Thompson, and E. D. Bauer, Ground-state wave function of plutonium in PuSb as determined via x-ray magnetic circular dichroism, Phys. Rev. B **91**, 035117 (2015).

[23] N. Magnani, R. Eloirdi, F. Wilhelm, E. Colineau, J. C. Griveau, A. B. Shick, G. H. Lander, A. Rogalev, and R. Caciuffo, Probing magnetism in the vortex phase of $PuCoGa_5$ by x-ray magnetic circular dichroism, Phys. Rev. Lett. **119**, 157204 (2017).

[24] S. K. McCall, M. J. Fluss, B. W. Chung, M. W. McElfresh, D. D. Jackson, and G. F. Chapline, Emergent magnetic moments produced by self-damage in plutonium, Proc. Natl. Acad. Sci. USA **103**, 17179 (2006).

[25] R. H. Heffner, K. Ohishi, M. J. Fluss, G. D. Morris, D. E. MacLaughlin, L. Shu, B. W. Chung, S. K. McCall, E. D. Bauer, J. L. Sarrao *et al.*, The search for magnetic order in δ-Pu metal using muon spin relaxation, J. Alloys Compd. **444–445**, 80 (2007).

[26] R. H. Heffner, G. D. Morris, M. J. Fluss, B. Chung, S. McCall, D. E. MacLaughlin, L. Shu, K. Ohishi, E. D. Bauer, J. L. Sarrao *et al.*, Limits for ordered magnetism in Pu from muon spin rotation spectroscopy, Phys. Rev. B **73**, 094453 (2006).

[27] F. Wilhelm, R. Eloirdi, J. Rusz, R. Springell, E. Colineau, J. C. Griveau, P. M. Oppeneer, R. Caciuffo, A. Rogalev, and G. H. Lander, X-ray magnetic circular dichroism experiments and theory of transuranium Laves phase compounds, Phys. Rev. B **88**, 024424 (2013).

[28] FLUO: Correcting XANES for self-absorption in fluorescence measurements, https://www3.aps.anl.gov/haskel/fluo.html (accessed 2-13-2023).

[29] XCOM: Photon Cross Sections Database, https://www.nist.gov/pml/xcom-photon-cross-sections-database (accessed 3-2-2023).

[30] K. T. Moore, G. van der Laan, R. G. Haire, M. A. Wall, and A. J. Schwartz, Oxidation and aging in U and Pu probed by spin-orbit sum rule analysis: Indications for covalent metal-oxide bonds, Phys. Rev. B **73**, 033109 (2006).

[31] G. van der Laan, K. T. Moore, J. G. Tobin, B. W. Chung, M. A. Wall, and A. J. Schwartz, Applicability of the spin-orbit sum rule for the actinide $5f$ states, Phys. Rev. Lett. **93**, 097401 (2004).

[32] G. van der Laan and B. T. Thole, Local probe for spin-orbit interaction, Phys. Rev. Lett. **60**, 1977 (1988).

[33] C. H. Booth, S. A. Medling, Y. Jiang, E. D. Bauer, P. H. Tobash, J. N. Mitchell, D. K. Veirs, M. A. Wall, P. G. Allen, J. J. Kas *et al.*, Delocalization and occupancy effects of $5f$ orbitals in plutonium intermetallics using L_3-edge resonant x-ray emission spectroscopy, J. Electron Spectrosc. Relat. Phenom. **194**, 57 (2014).

[34] R. P. Guertin, H. C. Praddaude, S. Foner, E. J. McNiff, and B. Barsoumian, Magnetic moment, susceptibility, and electrical resistivity of dilute paramagnetic palladium—Rare-earth alloys, Phys. Rev. B **7**, 274 (1973).